

정전기적으로 안정화된 실리카 입자 분산계의 미세구조 변화와 유변학적 거동

소재현, 양승만  
한국과학기술원 화학공학과

## **Microstructure and rheological behaviour of charge stabilized silica particle suspensions**

Jae-Hyun So, Seung-Man Yang

Department of Chemical Engineering, Korea Advanced Institute of Science and Technology

### **1. Introduction**

The flow behaviour and microstructure of particle dispersions have been studied intensively because of their practical significances in paints, ceramics, composite materials, electronic industry, coating process and so on. In particular, metal oxide suspensions have attracted considerable attention in the electronic industry [1]. Therefore, it is necessary to investigate the microstructural changes of particulate suspensions, and thereby to control the rheological properties under flow field. The flow characteristics of particulate suspensions can be controlled by the particle shape and size distribution, interparticle forces, and the volume fraction of the dispersed phase [1-3].

In general, silica particles in aqueous medium possess surface charge, and thus the silica particles are stabilized predominantly by electrostatic repulsion since the thickness of steric barrier is much smaller than the range of the electrostatic repulsion. The electrostatic repulsion can be controlled by varying ionic strength (or salt concentration) and pH. In the subsequent sections, the rheological responses of the silica suspensions were examined as functions of the particle size and volume fraction. In addition, we examined the microstructural transition of aqueous silica suspensions from liquid-like to solid-like structure by monitoring the storage ( $G'$ ) and loss ( $G''$ ) moduli for various particle volume fractions and salt concentrations.

### **2. Experimental**

Monodisperse silica particles were synthesized through the sol-gel method in ethanol medium (Oriental) proposed by Stöber *et al.* [4]. Tetraethylorthosilicate (TEOS;  $\text{Si}(\text{OC}_2\text{H}_5)_4$ ) and deionized water were used as reactants for preparation of the spherical silica particles with the aid of reaction catalyst, ammonium hydroxide. In order to prepare concentrated and mono-

disperse silica suspensions, hydrolysis and condensation reaction were carried step-wisely with time interval of 12 hrs by adding 0.57M TEOS sequentially [5], with the seed prepared by 0.57M TEOS, 0.35M  $\text{NH}_3$ , and 0.85M  $\text{H}_2\text{O}$ .

Charged stabilized silica suspensions, which have long-range repulsive interactions, were prepared in aqueous medium after surface modification with amino silane coupling agent, N-[3-(Trimethoxysilyl)propyl] ethylenediamine ( $((\text{CH}_3\text{O})_3\text{Si}(\text{CH}_2)_3\text{NHCH}_2\text{CH}_2\text{NH}_2)$ ). After the surface modification, silica particles were separated from the mixture by ultracentrifugation and re-dispersed in distilled water, of which the ionic strength was controlled by changing KCl concentration from  $10^{-3}$  to  $10^{-1}$ M.  $\zeta$ -potential of silica suspension was measured by electrophoretic light scattering (Brookhaven) and the results were also shown in Table 1. The rheological behaviour was monitored by an Advanced Rheometric Expansion System (ARES) under either steady or oscillatory shear flow in Couette geometry. The series of steady shear viscosity measurements were performed after samples were pre-sheared at a constant shear rate of  $0.025\text{s}^{-1}$  for 60s. Frequency sweep measurements in oscillatory shear flow were carried in the range of linear viscoelasticity determined by strain sweep test. All rheological measurements were conducted at a fixed temperature of  $25^\circ\text{C}$ .

### **3. Results and discussions**

The synthesized monodisperse silica particle was spherical and the average particle radii of S13 was  $108.52 \pm 5.52\text{nm}$  by TEM image. By fitting the viscosity data at extremely dilute concentrations to Einstein's theory, the densities of the prepared silica particles were determined as  $1.62 \times 10^{-3}\text{kg/m}^3$  for S13. This value of the particle density was very close to the previous results [6]. In addition, we also measured  $\zeta$ -potential through the electrophoretic mobility of the bare and surface modified silica particles using electrophoretic light scattering system. The  $\zeta$ -potential of each silica suspension were shown in Table 1 for various salt concentration in aqueous medium.

Shear viscosity of S13 suspension was plotted as a function of the shear rate for three different volume fractions of  $\phi = 0.371, 0.400, \text{ and } 0.427$  in Fig.1(a). In this plot, the salt concentration was adjusted to  $10^{-3}$  M. Typical shear thinning behaviour was observed for semi-dilute charge stabilized suspension of S13 for the salt concentration of  $10^{-3}$  M. It can be also seen that when the particle volume fraction was lower than 0.400, the zero-shear-rate viscosity was measurable. In order to examine the microstructure of S13 suspension with the salt concentration fixed at  $10^{-3}$  M, storage ( $G'$ ) and loss ( $G''$ ) moduli were measured as a function of the sweep frequency and the result is reproduced in Fig.1(b). Although both the storage and

loss moduli increased with the volume fraction, the increase in  $G''$  was steeper than that of  $G'$ . Therefore, at low volume fractions ( $\phi \leq 0.400$ ), the loss modulus  $G''$  was larger than or equal to the storage modulus  $G'$ . Also noted is that both the storage and loss moduli at low volume fractions increased monotonously with the frequency. However, as the volume fraction exceeded 0.400,  $G'$  and  $G''$  were nearly independent of the frequency. The behaviour of  $G'$  and  $G''$  as a functions of the particle volume fraction and frequency clearly indicates that the microstructure of S13 suspension changes from liquid-like structure to solid-like structure as the volume fraction increases. Furthermore, the overall feature of dynamic response ( $G'$  and  $G''$ ) was consistent with the previous shear viscosity behaviour.

The relative viscosity (i.e., suspension viscosity scaled by pure solvent viscosity) of charge stabilized suspensions at  $\phi = 0.400$  was given in Fig.2(a) for various salt concentrations. Also included in this plot for comparison is the relative viscosity of the 'hard sphere' suspension of HS13. It can be readily noted that as the salt concentration increased, the relative viscosity decreased and approached the viscosity of the hard sphere suspension. This clearly implies that the long-range repulsive force diminished with ionic strength and charged particles at high salt concentrations behaved like hard spheres. In particular, the change in shear viscosity as a function of the salt concentration was pronounced at low shear rates in which the interparticle forces were dominant rather than hydrodynamic forces imposed by the shear flow. In Fig.2(b), the storage and loss moduli were plotted as a function of the frequency for the same set of parameters as in Fig.2(a). It can be easily seen that the loss modulus is larger than the storage modulus when the salt concentration is above  $10^{-2}$  M. Also noted is that both the moduli decreased with the ionic strength. Indeed, at high salt concentrations, the charge stabilized suspensions displayed liquid-like behavior at the volume fraction  $\phi = 0.400$ . However, at a lower salt content, the trend was reversed. At a very low salt concentration  $[KCl] = 10^{-3}$  M, the storage ( $G'$ ) and loss ( $G''$ ) moduli of the S13 suspension with the volume fraction of  $\phi = 0.400$  showed very weak dependence on the frequency and  $G'$  is slightly larger than  $G''$ . Thus, at low salt concentrations, the charge stabilized suspensions exhibited solid-like behaviour, especially at low frequencies.

#### **4. References**

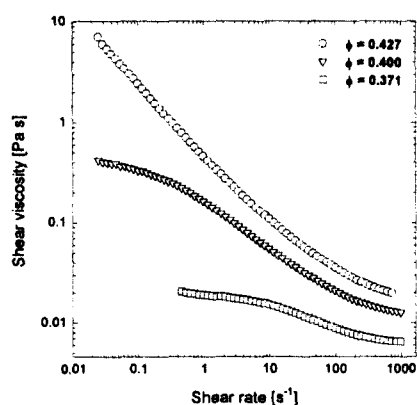
- [1] Th.F. Tadros, Adv. Colloid Interface Sci., **68** (1996) 97.
- [2] H.A. Barnes et al., An Introduction to Rheology. Elsevier Science, New York, 1989.
- [3] H.A. Barnes, J. Rheology, **33** (1989) 329.
- [4] W. Stöber, A. Fink, and E. Bohn, J. Colloid and Interface Sci., **26** (1968) 62.

[5] G.H. Bogush, M.A. Tracy, and C.F. Zukoski, *J. Non-Cryst. Solids*, **104** (1988) 95.

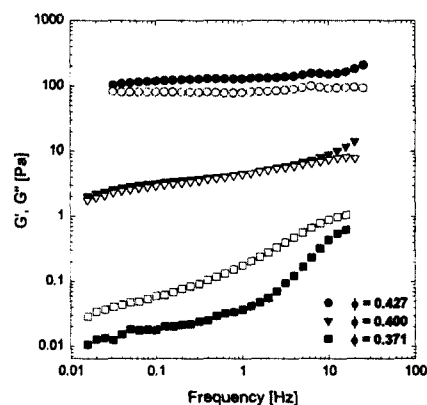
[6] J.-D. Lee, J.-H. So, and S.-M. Yang, *J. Rheology*, **42** (1999) 1117.

**Table 1.** pH and  $\zeta$  - potential of the silica particle suspensions

Sample	Bare silica suspension [KCl]=10 <sup>-3</sup> M	Surface modification with amino silane in aqueous solvent		
		[KCl]=10 <sup>-3</sup> M	[KCl]=10 <sup>-2</sup> M	[KCl]=10 <sup>-1</sup> M
S13	-52.7 ± 2.5 mV (pH = 9.13)	-48.6 ± 2.8 mV (pH = 8.86)	-39.4 ± 2.1 mV (pH = 8.48)	-12.8 ± 4.5 mV (pH = 8.45)

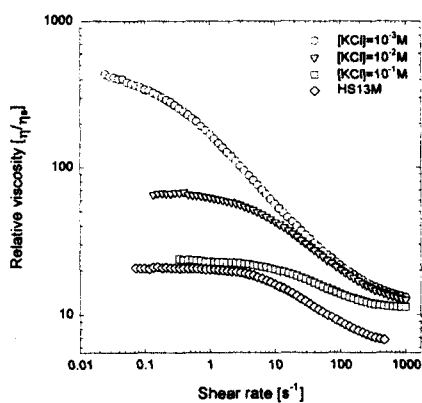


(a)

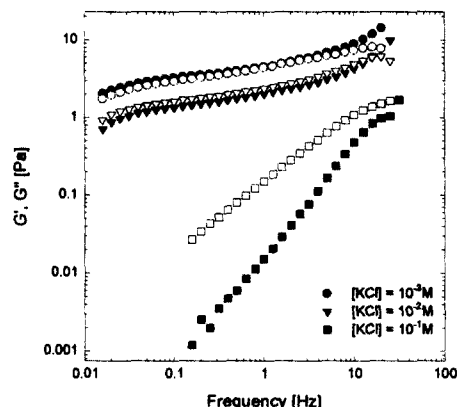


(b)

Figure 1. (a) Shear viscosity as a function of the shear rate, (b) Storage ( $G'$ ; filled symbol) and loss ( $G''$ ; open symbol) moduli as a function of the frequency for S13 with  $[KCl]=10^{-3}M$ .



(a)



(b)

Figure 2. (a) Relative viscosity as a function of the shear rate, (b) Storage ( $G'$ ; filled symbol) and loss ( $G''$ ; open symbol) moduli as a function of the frequency for S13 at  $\phi=0.400$ .